THE BELL SYSTEM TECHNICAL JOURNAL
Vol. 58, No. 4, April 1979
Printed in U.S.A.

Rapid Automatic Index Profiling of Whole-Fiber Samples: Part I

By L. M. BOGGS, H. M. PRESBY, and D. MARCUSE

(Manuscript received May 1, 1978)

A new interferometric method not requiring any sample preparation is presented for determining the refractive-index profiles of optical fibers. The whole fiber is immersed in index-matching oil and placed transversely under an interference microscope. The determination of the refractive index distribution for an arbitrary, circularly symmetric fiber core requires the solution of an integral equation. In this first of two papers on the subject, we describe a method which accomplished its solution by assuming that the fiber core consists of a large number of concentric circular cylinders of step-wise constant refractive index. The index distribution can then be obtained by determining the index values of each layer successively. The method has been applied to double- and single-pass interferometric arrangements which are being compared here. The single-pass method is reproducible to about 1 percent and provides the complete index distribution within minutes with the help of a computer-controlled video-analysis system. The results of this method are in excellent agreement with profiles obtained from polished slabs of the same fiber.

I. INTRODUCTION

Multimode optical fiber systems can achieve high bandwidth if the refractive index profile of the fiber core approximates very closely the theoretically predicted almost-parabolic shape. This poses the problem for the fiber fabricator of being able to produce preselected index profiles with high accuracy and also of being able to check whether the desired profile has actually been obtained. It is thus necessary to have measuring equipment capable of displaying the index profiles of fibers after manufacture quickly, accurately, and, if possible, nondestructively.

Means for measuring refractive index profiles by accurate interferometric techniques have previously been described.[1–3] However, the

most successful earlier technique, the slab method, requires elaborate sample preparation because a thin slice has to be cut out of the fiber and polished to a high degree of flatness and parallelism.

If the interferogram could be made by shining light not longitudinally but transversely through the fiber core, fiber preparation would become unnecessary, except for the need for preventing the fiber cladding from contributing a very large amount of fringe shift. This can be accomplished by submerging the fiber in index-matching oil. This general idea has been described in Ref. 4. A similar method has been used in Ref. 5, but the analysis used to extract the refractive index profile from the interferogram was restricted to power law profiles that can be characterized by two constants, the refractive index difference (between the maximum value at the core center and the cladding value) and the power law coefficient. Actual fibers have refractive index distributions that do not fit a simple power law. Most fibers at present have an index depression on axis and at the core boundary. But even the comparatively regular parts between core center and core boundary do not always conform to one definite power law profile. It is thus necessary to evaluate the transverse interferograms without assuming a particular functional shape for the index distribution. We describe such a method in this paper.

Because the fiber need not be cut and polished for transverse illumination, we call this procedure the "whole-fiber method."

The refractive index distribution $n(r)$ is related to the fringe shift pattern by an integral equation which we solve by replacing the function $n(r)$ by a staircase approximation. Our method is based on the assumption that the index profile is of rotational symmetry and neglects the effect of ray bending inside the core. The staircase approximation of the index curve is equivalent to an approximation of the original integral (of the integral equation) by a discrete sum and to solving the resulting system of coupled equations.

As a particular matter, the interferogram can be obtained in two different ways. If a single-pass interference microscope is available, the light beam need pass the fiber core only once. Some conventional microscopes can be equipped with an interference objective attachment that functions as an interferometer if the sample is placed on a mirror and the light beam is allowed to pass back and forth through it. This double-pass method suffers from the disadvantage that each ray is bent much more severely in passing the core twice, so that ray bending is no longer negligible. We present a comparison of the single- and double-pass methods in this paper. Furthermore, we describe an automated, computer-controlled video system for performing the interference measurements and data evaluation automatically and compare the results of the whole-fiber method with those of the more accurate slab method.

II. CIRCULAR INDEX METHOD: DOUBLE-PASS INTERFEROMETER

The experimental arrangement for double-pass interferometric observations is shown in Fig. 1. The double-pass interferometer has the advantage of being much cheaper than a commercial interference microscope because it utilizes an interference objective as an attachment to an ordinary microscope. A short section of the fiber is immersed in index matching oil and placed on a metallized optical flat serving as a mirror. The optical flat can be heated to achieve perfect match between the oil and the fiber cladding. The light source is a He-Ne laser whose beam is passed through a moving diffuser. A typical interferogram is shown in Fig. 2. The information needed to compute the refractive index distribution of the fiber core is obtained by measuring the displacement of one of the fringes from its straight level in the cladding.

Next, we describe how the information about the refractive index distribution is extracted from the interferogram. We assume that the light rays pass the fiber core without deflection, using only the fact that their phases are retarded according to the length of their optical paths. In addition, we assume that the fiber core consists of a large number of concentric rings each with a constant index of refraction. We now evaluate the index step by step beginning at the periphery and proceeding toward the center. Figure 3 shows clearly that it is possible to determine the index value of each ring if we use the fact

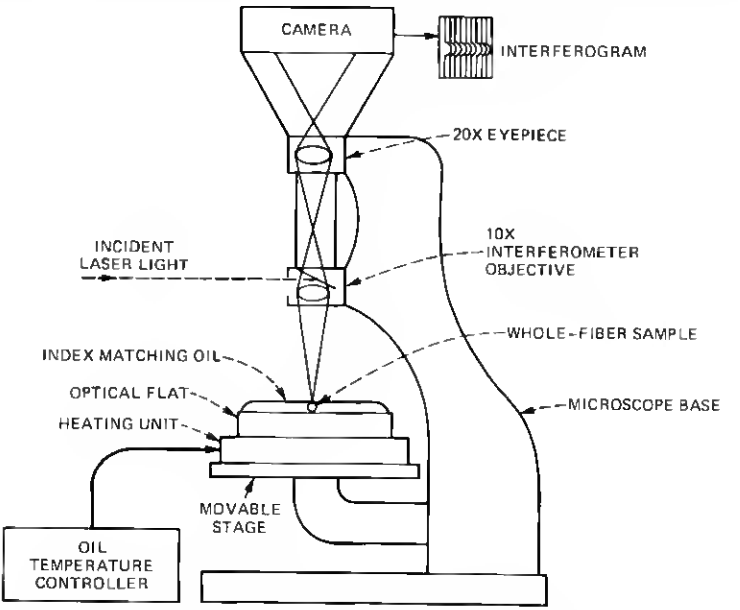

Fig. 1—Microscope set-up for making double-pass interferogram.

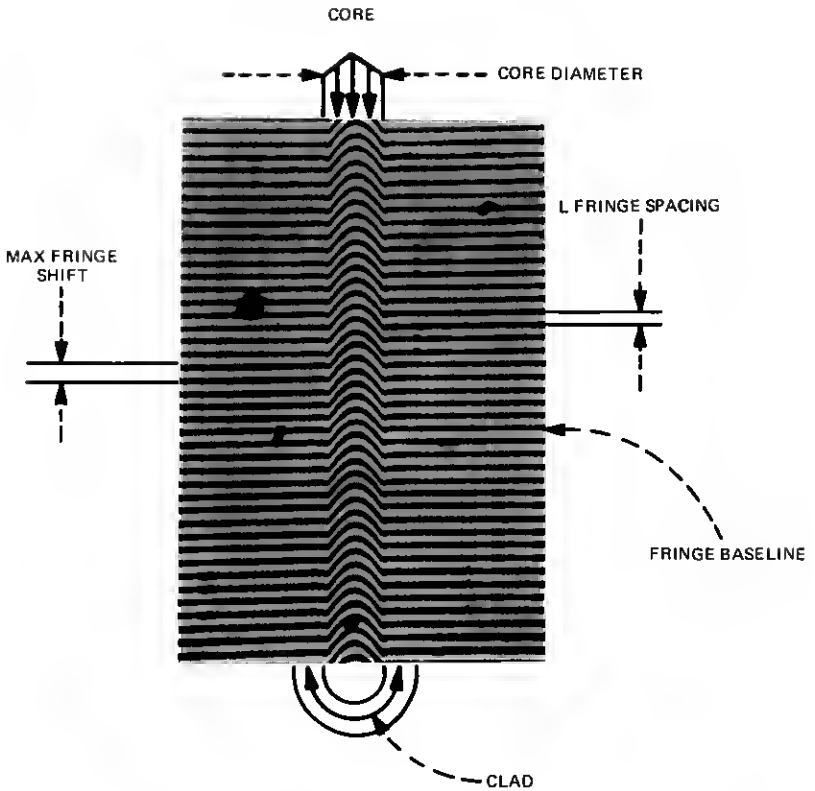

Fig. 2—Interferogram of whole-fiber sample obtained with double-pass set-up.

that the index values of all preceding rings are already known. We call this method of analysis the "circular index method."

The relationship between the relative optical phase shift ψ, fringe spacing L, and fringe shift Q is

$$Q(P) = \frac{L}{2\pi}\psi(P). \tag{1}$$

If we designate the radius of the Jth ring by $R(J)$ and note that the length of a single path through ring J is

$$S(P, J) = 2\{[R^2(J-1) - R^2(P)]^{1/2} - [R^2(J) - R^2(P)]^{1/2}\}, \tag{2}$$

we find that the double-path fringe shift through the core, passing through ring P on the horizontal axis, can be expressed as follows:

$$Q(P) = 2\frac{L}{\lambda}\left\{\Delta n(P)S(P, P) + \sum_{J=1}^{P-1}\Delta n(J)S(P, J)\right\}.$$

$\Delta n(J)$ is the difference between the refractive index value of ring J and the index of the cladding. Solving for $\Delta n(P)$ yields the relative

refractive index of ring P in terms of the phase shift (measured at the corresponding position) in terms of the relative index values of all preceding rings.

$$\Delta n(P) = \frac{1}{S(P, P)} \left\{ \frac{\lambda Q(P)}{2L} - \sum_{J=1}^{P-1} \Delta n(J) S(P, J) \right\}. \tag{3}$$

The iterative evaluation of this equation starts at an arbitrary radius large enough to ensure that $Q(1) = 0$ and $\Delta n(1) = 0$.

Note that the thickness of the rings, and hence the spacing at which the fringe shift values are sampled, need not be uniform. Our method of analysis also shows clearly that measurement errors must build up so that the refractive index near the fiber axis is known far less accurately than the index near the core boundary. This problem is aggravated by the fact that the weighting factor $1/S(P, P)$ in (3) becomes larger closer to the core center. However, these features of our method seem unavoidable since the same type of error build-up

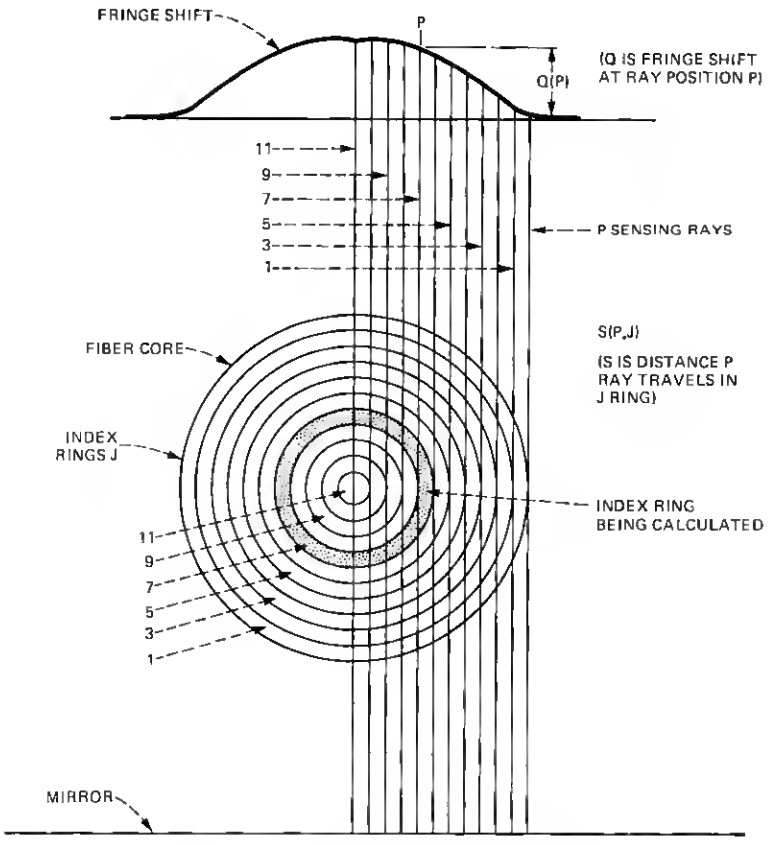

Fig. 3—Circular-index calculation scheme.

occurs also in another method (described in a companion article[6]), which is based on an analytical solution of the integral equation. Figure 4 shows a typical plot of Δn vs radial position together with a power law curve fitted to the data. Four points near the fiber core center are omitted from the curve-fitting program, since they clearly did not conform to a simple power law.

III. CIRCULAR INDEX METHOD: SINGLE-PASS INTERFEROMETER

The circular index method, previously discussed, ignores bending of the sensing light rays as they pass through the core on their way to the mirror and on their return through the fiber. In actuality, ray bending does occur, and the amount of bending is readily computed by successive applications of Snell's law. Figure 5 shows the rays vertically incident from the top of the core and tilted from the vertical direction on the return from the mirror. This figure shows clearly that

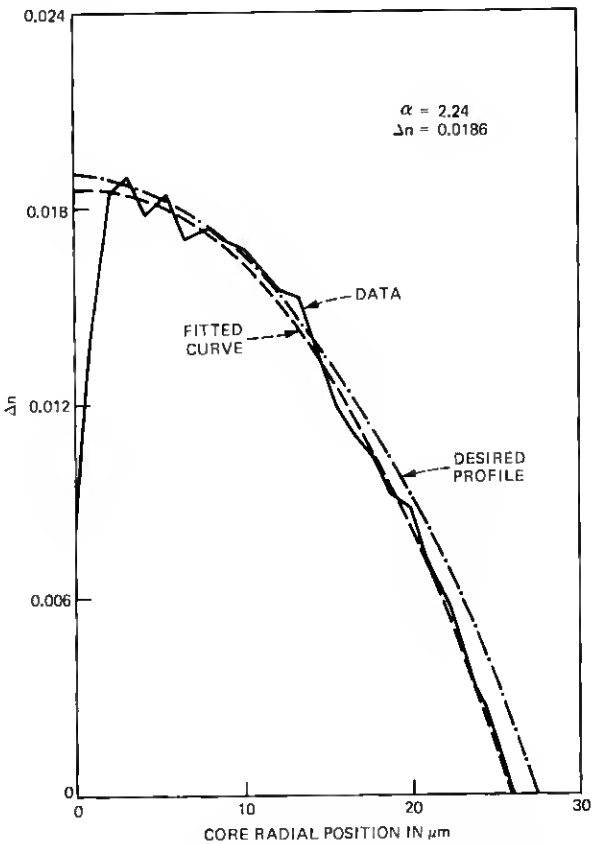

Fig. 4—Index profile obtained from double-pass interferogram.

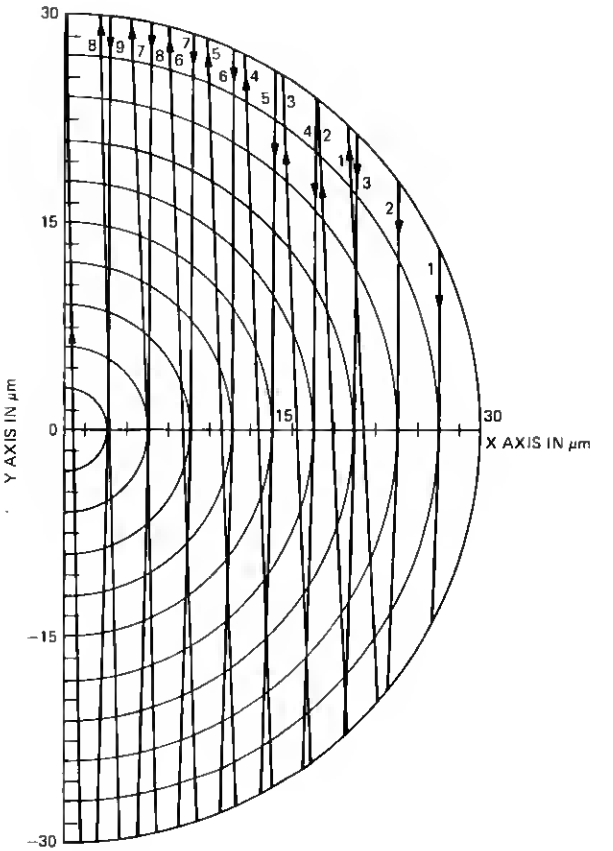

Fig. 5—Ray bending of incident and reflected rays in double-pass arrangement.

significant ray displacement occurs, particularly near the core boundary. If single-pass interferometry of the Mach-Zender type were used, the sensing ray would pass through the fiber only once. The amount of ray bending in this case is shown in Fig. 6. The point at which the ray exits the core is translated only about ⅛ the distance experienced in the two-pass case. Furthermore, the change in the exit angle caused by the core is only about ½ the amount of the two-pass case.

Although an α of 1.0 was assumed for the calculated ray bending effects shown in Figs. 5 and 6, equally significant ray bending occurs for other α values, for example, for $\alpha = 2$. The ray displacement shown in Fig. 5 suggests that the double-pass method tends to eliminate fine structure from the interferogram and hence from the refractive index curve. Fibers made by modified chemical vapor deposition typically

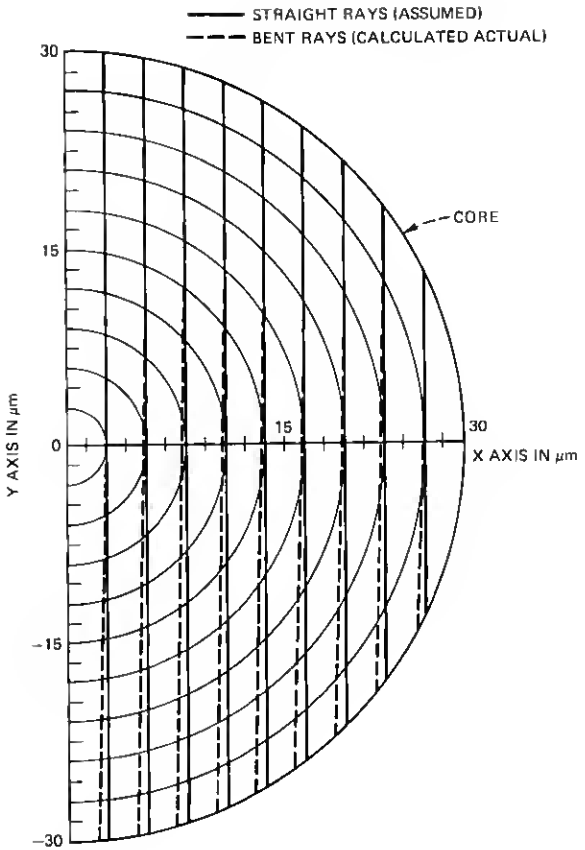

Fig. 6—Ray bending of incident rays in single-pass arrangement.

show the deposition layers if high resolution methods are used. Such fine structure is usually seen with the single-pass method, particularly near the fiber axis.

A comparison of double-pass and single-pass interferograms of the same fiber sample is shown in Fig. 7. The different magnification used for the two methods is inherent in their practical realization. Interference objectives for conventional microscopes are at present not available with high magnification. Interference microscopes, on the other hand, are equipped with high power objectives. Close scrutiny of Fig. 7 reveals that the single-pass interferogram shows the central dip[7] in the fiber core while this feature is less obvious from the double-pass interferogram. The more sophisticated single-pass method, using a

high precision interference microscope, is a definite necessity if fine detail of the refractive index distribution is to be resolved. To take full advantage of the inherently rapid nature of this profiling method makes it desirable to automate the measurement. A description of the automated equipment is presented in the following section.

IV. AUTOMATIC SINGLE-PASS PROFILING

The experimental arrangement for automatic single-pass profile measurements is shown in Fig. 8. The heart of the system is a Leitz dual-beam, single-pass, transmission interference microscope. This instrument is essentially a combination of two microscopes and an interferometer in such a way that the magnified image of the object appears together with interference fringes. The interference microscope has been extensively used to perform precise refractive index profiling of optical fibers by examining polished slab samples.[1-3] Techniques have also been developed to make measurements of the fringe

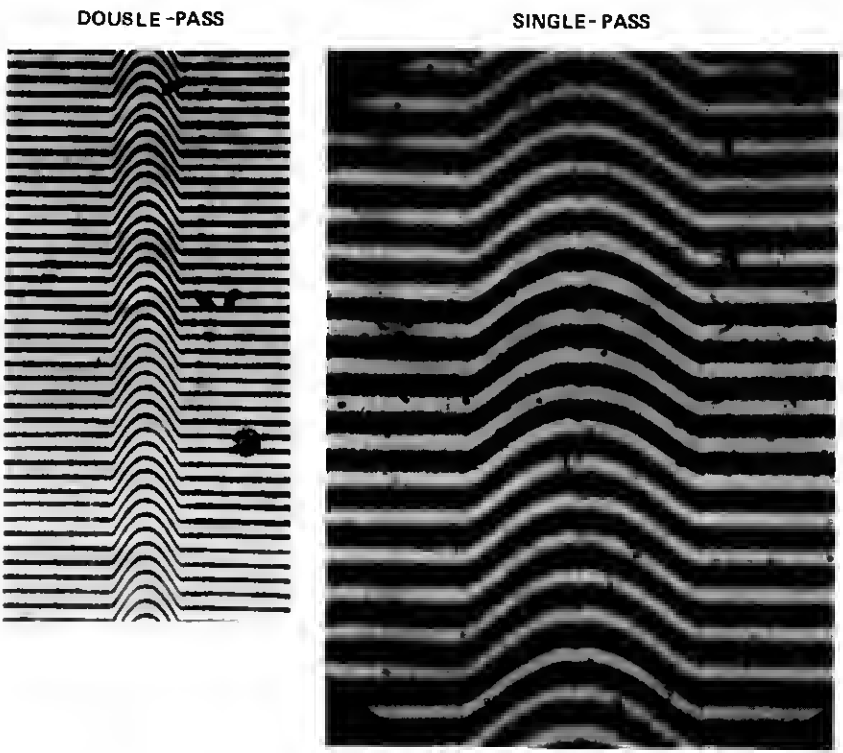

Fig. 7—Comparison of double-pass and single-pass interferograms of the same fiber sample.

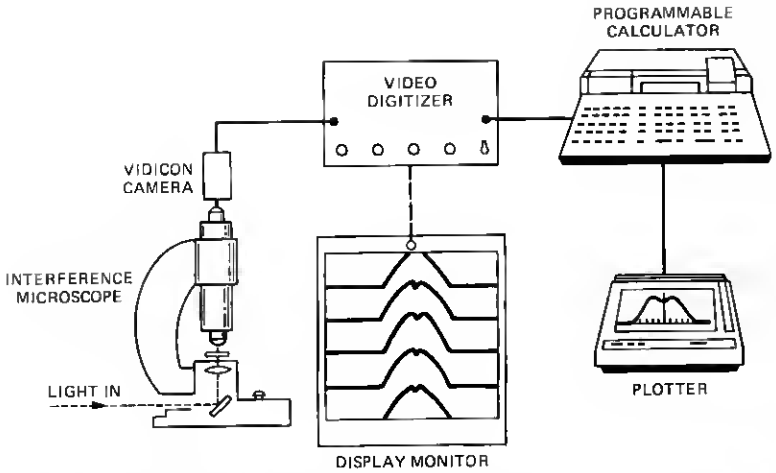

Fig. 8—Elements of the set-up to perform automatic-refractive index profiling of whole-fiber samples with a single-pass interference microscope and a video analysis system.

displacements directly in the microscope's output field[3, 8-11] without the time-consuming need to process photographs.

In our application, a short length of fiber (~1 cm) is inserted into index-matching oil in the sample arm of the microscope. However, if desired, the unbroken fiber could be placed under the microscope. A similar thickness of matching oil is placed in the reference beam. We found that an excellent match to the cladding could be achieved at an observation wavelength of $\lambda = 0.9$ μm with matching oil of index $n = 1.457 \pm 0.0005$; no heating of the oil was employed.

The subsequent measurement procedure is similar to that of Ref. 9 and involves video detection and digitization of the interference fringes under computer control. The output field of the microscope is detected with an infrared-enhanced, silicon-target vidicon whose electronics were modified to optimize signal stability and to reduce voltage drift to minimum levels. The video signal is sent to a video digitizer that has the capability of addressing and encoding discrete picture elements in the television frame. The digitizer resolves 480 picture elements on the Y axis and 512 elements on the X axis. The X and Y position data inputs are provided by the 16-bit duplex input/output (I/O) interfaces of a Hewlett Packard 9825A computer. Encoding is to 8 bits or 256 gray levels and the digitized video is received by the calculator as 8 bits, parallel binary.

The digitizer also incorporates a video output display which permits the observation of the scene being processed and the monitoring of the encoding on the same screen. Figure 9 is a photograph of the display showing a sample of an index-matched graded-index fiber observed at

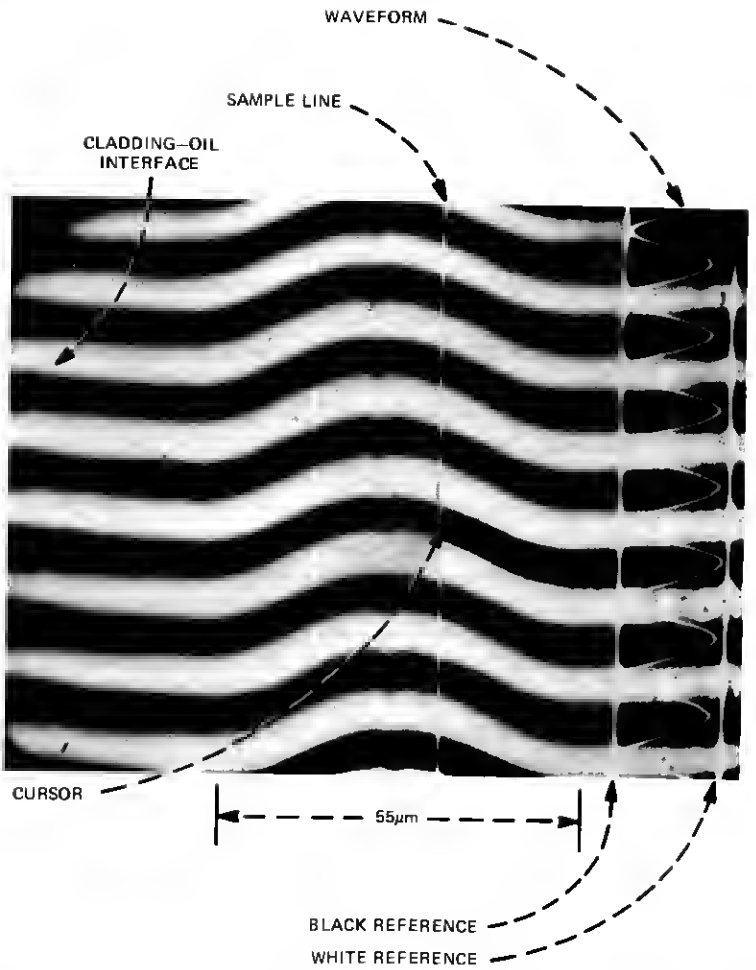

Fig. 9—Photograph of monitor showing graded-index fiber and associated encoding display of sample line, cursor, and intensity waveform. Note that the interface between the matching oil and the cladding is barely visible, indicating a good match.

a wavelength of $\lambda = 0.9$ μm. Location of the point being encoded is indicated by a dot cursor and the gray-scale value for all Y elements along a sample line at the selected X positions is displayed as a waveform at the side of the monitor screen. Care is taken when setting up the sample to ensure that the axis of the fiber is normal to the vidicon scanning axis and that the straight fringes in the cladding region lie nearly parallel to the scanning axis. Residual fringe tilt relative to the scan lines is compensated for by the data evaluation program.

The objective of the encoding process is to accumulate intensity-vs-position data so that the displacement of a fringe from its cladding

level can be determined accurately as a function of radial position. This is accomplished by a new automatic, rapid, fringe finding and tracking procedure the details of which are presented in a companion paper.[6] Having determined the fringe displacement, the computer calculates Δn by the method described in a previous section and then plots the index profile along with coordinates and labeling on an XY plotter.

The computer's program then determines a best-fit power-law (α) curve to the index profile. Since the profiles of most currently fabricated fibers contain perturbations, mainly in the form of a central index depression and tails at the core-cladding interface, the program provides means of ignoring these regions, which clearly do not follow the power law, by selecting the portions of the profile over which a fit is to be determined. The coordinates of the limits of these regions are entered into the computer which then proceeds to fit four variables to the given profile, viz., the core radius, the shift of the center of the core, the maximum index difference between core and cladding, and the α parameter. The program also determines a "fitting error" to provide a measure of how well the α curve approximates the measured profile. At the conclusion of the fitting program, the values of the various parameters are printed out and a best-fit α curve is drawn by the plotter.

The above procedure was used on eight different GeO_2-doped fibers fabricated by modified chemical vapor deposition (MCVD). The results, giving the fitted values as described above, are presented in Table I

Table I—FIT parameter comparison

Fiber ID	Δn	Core-radius (μm)	Alpha	FIT Error (%)	FIT Bounds (μm)
20G61BX					
Slab	0.0202	22.29	2.23	1.5	5–20
Whole	0.0190	21.39	2.36	2.3	5–20
14F305B					
Slab	0.0183	27.67	2.32	1.1	5–25
Whole	0.0174	27.07	2.35	0.8	5–25
20W97A					
Slab	0.0227	27.89	1.49	1.0	5–25
Whole	0.0220	26.69	1.57	1.0	5–25
20W99A					
Slab	0.0230	27.22	1.48	0.8	8–25
Whole	0.0221	27.04	1.45	0.8	8–25
19F53BX					
Slab	0.0207	22.94	2.17	0.9	4–21
Whole	0.0194	22.31	2.39	1.9	4–21
15F309B					
Slab	0.0184	25.60	2.25	1.2	5–22
Whole	0.0185	24.76	2.43	2.7	5–22
14A186B					
Slab	0.0212	26.74	1.70	0.6	12–25
Whole	0.0228	26.94	1.75	0.6	12–25
19A118A					
Slab	0.0094	24.95	2.06	0.7	3–22
Whole	0.0089	24.90	2.04	1.47	3–22

across the rows labeled "Whole." Also shown are the limits of the fitted region. It is important to note that, since these profiles are not ideal α distributions, the value of α depends on the limits of the region over which the fit is made. We have found that slight changes of these limits can affect the α value by about 5 percent.

The reproducibility of the measured profile is limited mainly by the build-up of errors in the integration scheme, an effect which is treated in detail in Ref. 6. Resulting variations of the index were consistently found to be a few parts in 10^4, in excellent agreement with a theoretical analysis of this effect.[6]

To check these results and establish the validity of this method of index-profiling, we prepared polished slabs of the same fiber samples and measured their profiles by the already established techniques of interference microscopy.[2] These measurements utilized the same automatic video analysis system with appropriate changes in the scanning and index evaluation procedures tailored to the slab geometry.[9] The experimental reproducibility of the profile for the slab samples is limited mainly by noise on the video signal. Variations in the index

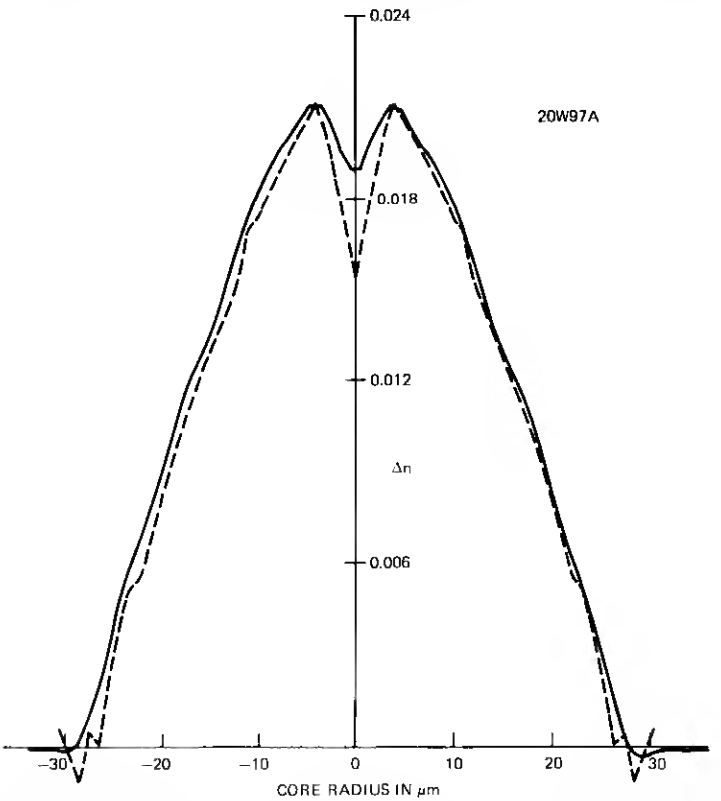

Fig. 10—Comparison of whole-fiber profile (broken line) with slab profile (solid line).

amount to a few parts in 10^5. This is about an order of magnitude better than the whole-fiber method which, as mentioned, is inherently limited by error build-up. This level of accuracy, however, reflects only the repeatability of the measurement and the absolute error depends upon a precise knowledge of the sample's thickness and its degree of flatness.[10]

For comparison with the whole-fiber results, the α fit to the slab profiles were made over the same region. Results obtained by the slab method are shown in Table I across the rows labeled "Slab." The agreement is seen to be very good, with the average difference of the maximum Δn values and the α values being about 4 percent and the average difference of the core radii being about 2 percent. Generally, the absolute values of Δn and core radii for the slabs are slightly larger than the whole fiber results. These discrepancies, however, are understandable because they are within the experimental precision of the

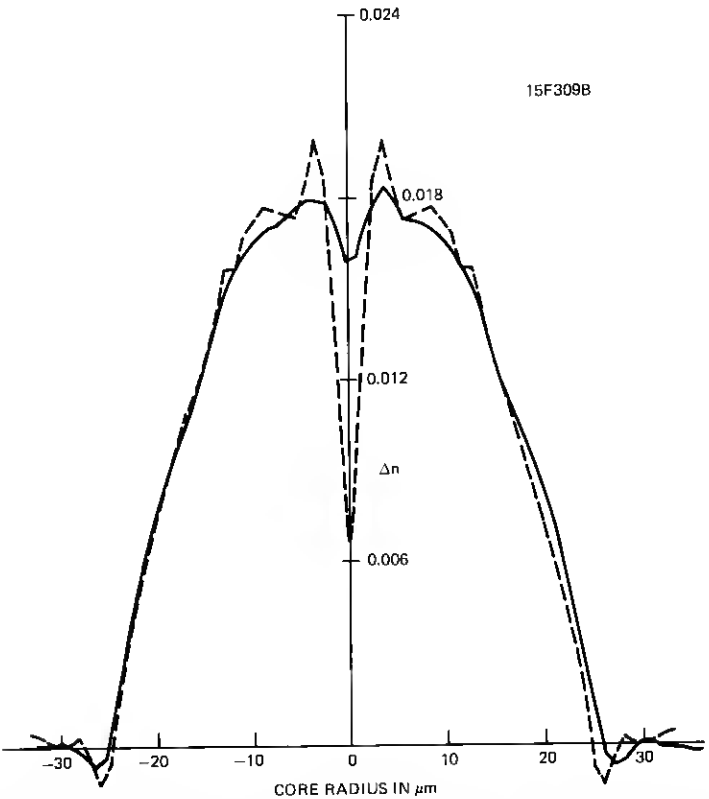

Fig. 11—Same as Fig. 10, but for a second fiber. The discrepancy of the radii on the right can be due to a slightly elliptical core which would be detected by the slab technique but not by the whole-fiber method since the latter assumes circular symmetry.

thickness measurements for the slabs (about 5 percent), which will affect the Δn level, and the error introduced by the lack of a perfect index match to the cladding of the whole fibers, which tends to reduce their observed radii (if the matching oil has a slightly higher index than the cladding). There is also the complication of focussing effects due to the boron layer, which can act differently for both cases, changing the apparent radius. In addition, the whole fiber analysis assumes circular symmetry, whereas the slab results are distinct for each side of the core. Thus, lack of circular core will not be apparent in the whole fiber results.

Besides the good agreement of the fitted data, the details of the index profiles themselves are in excellent correspondence. Generally, distinctive features of the profiles are present in both cases, as can be seen in the three typical profiles shown in Figs. 10 to 12. A tendency of the whole-fiber technique is to display more clearly the layers in the

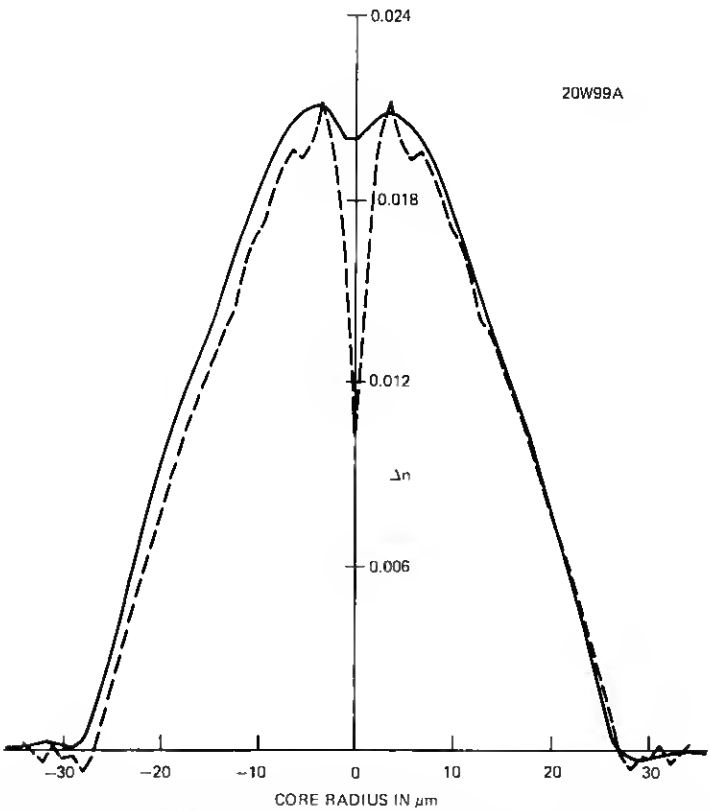

Fig. 12—Same as Fig. 10, but for a third fiber. The whole-fiber method tends to emphasize structural details, as explained in the text.

fiber core which exist especially near the axis. This is due to the fact that the whole-fiber method tends to magnify any fluctuations, and consequently also systematic ones, near the core center. The central index depression is also resolved to a greater degree by the whole-fiber method since this region, in the slab case, possesses a large index gradient which cannot be resolved by the interference fringe passing through it. The depth of the depression, as displayed by the whole-fiber profile, depends on how closely a vertical scanning line comes to the axis of the fiber, accounting for the variations that are observed in this region of the profiles.

The whole-fiber method shows itself to be a viable technique to measure index profiles, although with somewhat less inherent attainable precision than the slab method. Its main advantage of not requiring sample preparation and thus providing information within minutes should make it a very valuable diagnostic tool. Profile information can now be rapidly provided to allow adjustments in fiber-preform fabrication parameters to attain more ideal index distributions. Fibers can now also readily be evaluated, rated, and selected nondestructively for specific applications, depending upon the quality of their profiles, almost immediately upon production. In addition, the method also has the capability of providing information on core and cladding diameter values.

REFERENCES

1. C. A. Burrus and R. D. Standley, "Viewing Refractive-Index Profiles and Small-Scale Inhomogeneities in Glass Optical Fibers: Some Techniques," Appl. Opt., *13* (1974), p. 2365.
2. H. M. Presby, W. Mammel, and R. M. Derosier, "Refractive Index Profiling of Graded Index Optical Fibers," Rev. Sci. Instr., *47* (1976), p. 348.
3. H. M. Presby and I. P. Kaminow, "Binary Silica Optical Fibers: Refractive Index and Profile Dispersion Measurements," Appl. Opt., *15* (1976), p. 3029.
4. M. E. Marhic, P. S. Ho, and M. Epstein, "Nondestructive Refractive-Index Profile Measurement of Clad Optical Fibers," Appl. Phys. Lett., *26* (1975), p. 574.
5. M. J. Saunders and W. B. Gardner, "Nondestructive Interferometric Measurement of the Delta and Alpha of Clad Optical Fiber," Appl. Opt., *16* (1977), p. 2368.
6. H. M. Presby, D. Marcuse, L. Boggs, and H. W. Astle, "Rapid Automatic Index Profiling of Whole Fiber Samples: Part II," B.S.T.J., this issue, pp. 883–902.
7. H. M. Presby, "Axial Refractive Index Depression in Preforms and Fibers," Fiber and Integrated Optics, *2*, No. 2.
8. H. M. Presby and H. W. Astle, "Optical Fiber Index Profiling by Video Analysis of Interference Fringes," Rev. Sci. Instr., *49* (1978), p. 339.
9. H. M. Presby, D. Marcuse, and H. W. Astle, "Automatic Refractive Index Profiling of Optical Fibers," Appl. Opt., *17* (1978), p. 2209.
10. J. Stone and R. M. Derosier, "Elimination of Errors due to Sample Polishing in Refractive Index Profile Measurements by Interferometry," Rev. Sci. Instr., *47* (1976), p. 885.
11. B. C. Wonsiewicz, W. G. French, P. D. Lazay, and J. R. Simpson, "Automatic Analysis of Interferograms: Optical Waveguide Refractive Index Profiles," Appl. Opt., *15* (1976), p. 1048.